

Research Article

Achraf El Mohajir, Jimena Castro-Gutiérrez, Alain Celzard, Franck Berger, Vanessa Fierro*, and Jean-Baptiste Sanchez*

Relevance of pore network connectivity in tannin-derived carbons for rapid detection of BTEX traces in indoor air

<https://doi.org/10.1515/rams-2025-0103>
received August 08, 2024; accepted March 27, 2025

Abstract: This study showcases the exceptional detection capabilities of a silicon-based micro-analytical device engineered to identify low concentrations of BTEX (benzene, toluene, ethylbenzene, and xylene) in indoor air, with a focus on the critical role of connectivity within the adsorbent material. Two micro-mesoporous carbons were synthesized using an eco-friendly method, differing primarily in their mesoporosity: one with an ordered structure (OMC) and the other with a disordered, interconnected porous network (DMC). The high pore connectivity of the DMC significantly enhanced BTEX accessibility to micropores, leading to superior preconcentration and detection performance, even under realistic conditions with 60% relative humidity at 25°C. The DMC-based system achieved the detection of BTEX compounds at ppb levels within a short analysis time (~10 min), demonstrating the importance of pore network connectivity in the adsorption process. This study underscores the potential of DMC as a highly efficient adsorbent for detecting volatile organic compounds in challenging indoor environments, where high connectivity within the porous structure is key to achieving outstanding performance.

Keywords: BTEX detection, porous materials, indoor air pollution

* Corresponding author: **Vanessa Fierro**, Université de Lorraine, CNRS, IJL, F-88000, Vosges, Épinal, France, e-mail: vanessa.fierro@univ-lorraine.fr, tel: +33 3 72 74 96 77

* Corresponding author: **Jean-Baptiste Sanchez**, Université Marie et Louis Pasteur, CNRS, institut FEMTO-ST, F-25000, Doubs, Besançon, France, e-mail: jbsanche@femto-st.fr, tel: +33 3 63 08 24 93

Achraf El Mohajir, Franck Berger: Université Marie et Louis Pasteur, CNRS, institut FEMTO-ST, F-25000, Doubs, Besançon, France

Jimena Castro-Gutiérrez: Université de Lorraine, CNRS, IJL, F-88000, Vosges, Épinal, France

Alain Celzard: Université de Lorraine, CNRS, IJL, F-88000, Vosges, Épinal, France; Institut Universitaire de France (IUF), F-75231, Paris, France
ORCID: Vanessa Fierro 0000-0001-7081-3697

1 Introduction

Volatile organic compounds (VOCs), even at extremely low concentrations in indoor air, severely affect human health. Consequently, it is imperative to monitor air quality and gain insights into pollutant emissions. Among VOCs, BTEX compounds (*i.e.*, benzene, toluene, ethylbenzene, and xylenes) are probably the most hazardous, primarily due to their carcinogenic effect [1]. Indoor concentrations of these compounds can vary from 0.1 to 50 ppb, requiring highly sensitive detection equipment [2–4]. The reference method for monitoring BTEX is gas chromatography, often preceded by a passive or active sampling step. Recently, significant efforts have been devoted to develop innovative miniaturized gas chromatographs for *in situ* identification and discrimination of pollutants in complex mixtures [5,6].

To meet the sensitivity challenge, preconcentration of the target compounds is necessary, and the key point is to identify a suitable adsorbent offering a rapid and reversible adsorption–desorption process. Porous materials, including zeolites, activated carbons (ACs) and metal organic frameworks (MOFs), have been explored for their potential in mitigating VOCs in ambient air [7–9]. Additionally, they have been explored for incorporation into preconcentration units to improve the sensing responses of a micro-gas chromatograph (μ -GC) prototype [9]. Although ACs are widely employed as carbon-based adsorbents for VOCs, they exhibit high adsorption affinities [10,11], limiting their use as preconcentrators in micro-systems. This limitation arises from the exceptionally high temperatures required for VOC desorption (~300°C). In a previous study, we demonstrated that using a non-activated micro-mesoporous carbon (MMC) in a micro-analytical prototype, considered as a μ -GC, provided better adsorption capacities when used as preconcentrator in comparison with DaY zeolite and MIL-101(Cr) MOF [12].

Our investigation begins with a detailed analysis of the textural properties of the selected materials, followed by an assessment of their water affinity through water

adsorption isotherms. We then explore the adsorption/desorption capacities of each adsorbent material, utilizing the μ -GC prototype to preconcentrate indoor air pollutants, with a specific focus on a BTEX mixture as representative aromatic indoor air pollutants. Additionally, we examine the influence of relative humidity (RH) on the performance of these materials, replicating typical indoor air conditions.

In this context, our findings emphasize the crucial role of high pore network connectivity in the adsorption process. The study highlights how this connectivity significantly enhances the detection efficiency of indoor air pollutants, even at trace concentrations, under realistic environmental conditions. By demonstrating the superior performance of disordered micro-mesoporous carbons (DMC) with highly interconnected porous networks, we underline the transformative potential of these materials in environmental monitoring applications, particularly for indoor air quality assessment. This work paves the way for future innovations in VOC detection technologies, where the design of adsorbent materials with optimized pore structures could lead to significant advancements in environmental sensing and public health protection.

2 Experimental

2.1 Adsorbents

Tannin-derived MMCs were synthesized using a simple, fast, and green mechanosynthesis method described elsewhere [13]. Briefly, the mechanical mixing of mimosa tannin (T), a surfactant (Pluronic F127[®], P) and water (W), followed by a thermal treatment up to 900°C under nitrogen atmosphere, allows producing MMC.

Changes in surfactant concentration in aqueous solutions lead to different phases. In this three-component mixture (T, P, and W), it was shown that changing the P:W mass ratio resulted in either a disordered mesoporous structure or an ordered one with a 2D hexagonal geometry [13]. During the thermal treatment, microporosity is developed and P and W are removed (P is fully removed at ~400°C), creating the mesopores, thus resulting in the MMC material. Specifically, a T:P:W mass ratio of 2:2:2 was used to obtain a disordered mesoporous carbon (DMC), while a ratio of 2:0.75:1.75 produced an ordered mesoporous carbon (OMC).

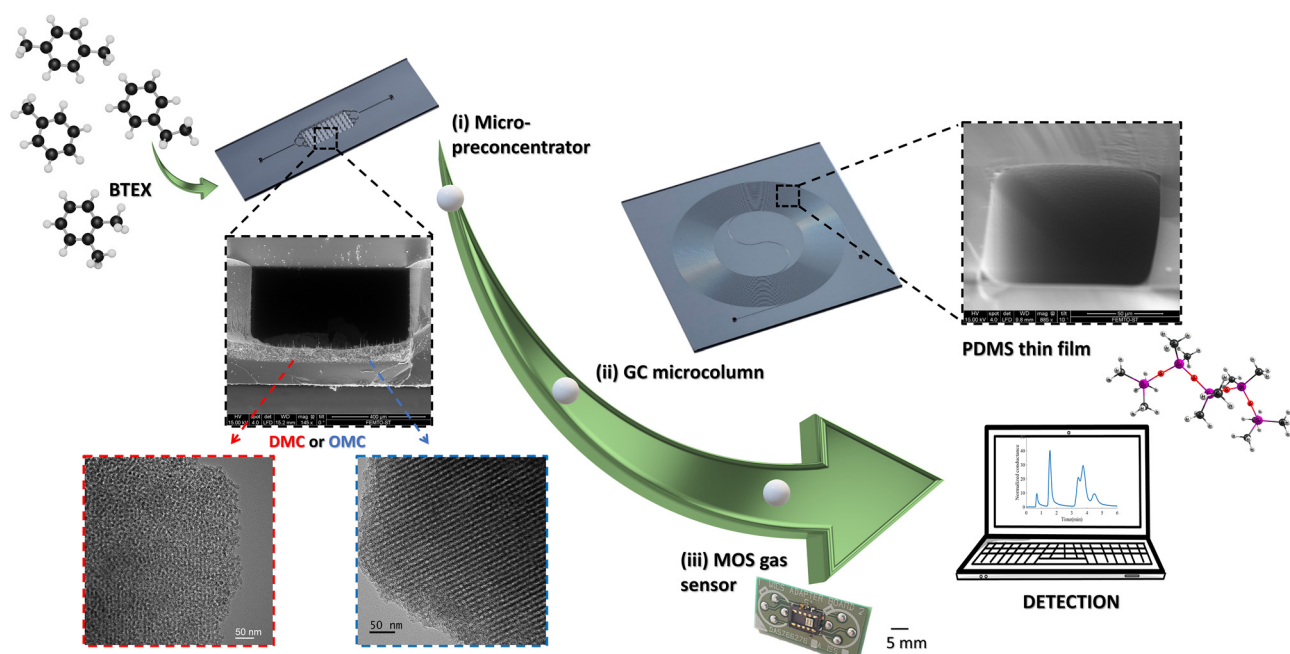


Figure 1: Design diagram of the micro-GC prototype: (i) silicon gas micropreconcentrator coated with either the DMC or the OMC material, (ii) silicon gas chromatography microcolumn coated with PDMS stationary phase, and (iii) metal oxide semiconductor gas sensor. The inserts illustrate the cross-sectional SEM images, showcasing the carbon layer and the 100 nm PDMS stationary-phase film. DMC and OMC TEM images are also shown to illustrate the mesoporous structure of each material.

A detailed physicochemical characterization of these MMCs is reported elsewhere [13,14], showing that the main difference between them lies in the properties of their mesoporous structure, since Raman spectra analysis revealed that both MMCs consist of poorly crystallized (amorphous) carbon due to the use of the same bio-sourced precursor [13]. Argon (Ar) and hydrogen (H₂) adsorption–desorption isotherms of the MMC materials were obtained at -186 and -196°C, respectively, using a Micromeritics ASAP 2020 automatic system equipped with a helium cryostat to control the temperature for Ar isotherms and liquid nitrogen to control the temperature for H₂ isotherms. The apparent surface area (A_{BET}) was calculated from Ar isotherms following the Rouquerol criteria [15], while the 2D non-local density functional theory (2D-NLDFT) for heterogeneous surfaces was applied simultaneously to Ar and H₂ adsorption isotherms using the SAIEUS® software (Micromeritics) to obtain the differential and cumulative pore size distributions (PSDs).

Furthermore, the morphologies of both adsorbents were examined via transmission electron microscopy (TEM) measurements conducted with a JEM-ARM 200 F Cold FEG TEM/STEM operating at 200 kV. The instrument was equipped with a spherical aberration (Cs) probe and image correctors, providing a point resolution of 0.12 nm in TEM mode and 0.078 nm in STEM mode.

2.2 Prototype overview and testing procedure

Figure 1 illustrates the layout of the micro-analytical units constituting the prototype. The device is composed of a gas micro-preconcentrator connected to a 5 meter long silicon-etched spiral gas chromatographic micro-column and a commercial tin oxide-based gas sensor [16]. These individual units are interlinked using capillaries and a six-way valve equipped with a 200 μL sampling loop. The interior of the gas micro-preconcentrators was coated with a thick, uniform layer of each selected adsorbent following the procedure described elsewhere [16]. Briefly, this process involves filling each micro-preconcentrator under vacuum with a dispersion of the adsorbent in a suitable solvent (ethanol) until it was completely filled. The solvent is then evaporated at room temperature, leaving behind a deposited layer of the adsorbent inside the micro-preconcentrator. The quantity of adsorbent weighed post-deposition in each micro-preconcentrator was 0.7 ± 0.1 and 0.4 ± 0.1 mg for OMC and DMC, respectively. The inner wall of the gas chromatographic micro-column was coated with a

thin film (100 nm) of polydimethylsiloxane (PDMS) stationary phase, facilitating the separation of all desorbed BTEX compounds. Detection was achieved using a miniaturized tin oxide (SnO₂)-based gas sensor (MICS-5524) purchased from SGX SENSORTECH. In all experiments, the sensor was powered with a 2.5 V voltage, resulting in a sensitive surface temperature of approximately 350°C. The sensor response was based on changes in the electrical resistance of the metal oxide material, caused by the chemical reaction between the eluted biomarkers from the GC micro-column and the sensitive surface, serving as the sensing signal for the prototype. At this operating temperature, the gas sensor provides a near-instantaneous response time, essential for its performance as a chromatographic detector. The morphology (surface and cross-sectional views) of adsorbent and PDMS stationary phase was observed by scanning electron microscopy (SEM) with a Dual Beam SEM/FIB FEI Helios 600i 98 microscope.

The VOCs were generated using Teflon tubes placed inside permeation ovens (Calibrage Model PUL 200). Each permeation tube contains a permeable membrane that releases a controlled flow of chemical vapor from the pure liquid analyte sealed within. At a constant temperature, the analyte vapor is emitted at a very low but stable rate (in $\text{ng}\cdot\text{min}^{-1}$) through the tube wall. The emission rate is determined by monitoring the tube's weight loss over time. The initial concentrations of vapors in the synthetic air (mixture of nitrogen 80% and oxygen 20% with low levels of water (~2% RH at 25°C)) flow were as follows: 2.4 ± 0.1 ppm for benzene, 3.1 ± 0.1 ppm for toluene, 1.6 ± 0.1 ppm for ethylbenzene, 2.5 ± 0.1 ppm for *o*-xylene, and 2.9 ± 0.1 ppm for *p*-xylene. Humidity levels were controlled using a Bronkhorst CEM-System (controlled evaporation and mixing). For all the experiments, the testing procedure involved the simultaneous adsorption of all BTEX compounds on the selected adsorbent at room temperature (~25°C) and under synthetic air gas flow rate of 40 $\text{mL}\cdot\text{min}^{-1}$ for 5 min. Then, all BTEX compounds were desorbed by applying a thermal flash at 220°C using an ULTRAMIC® Advanced Ceramic Heater positioned at the back of the micro-preconcentrator, with a PID temperature controller regulating the heating rate at 5.5°C·s⁻¹. The desorbed BTEX compounds were then injected into a silicon-etched GC μ -column through a sample loop for separation prior to their reaction with the sensitive surface of a miniaturized tin oxide gas sensor. The GC μ -column was maintained at a constant temperature of 35°C throughout the experiment and an air carrier gas flow rate of 7 $\text{mL}\cdot\text{min}^{-1}$ was used, corresponding to the optimal conditions for the separation of BTEX compounds. The sensor response was calculated as $S = (G - G^0)/G^0$, where G is the conductance under the BTEX compounds and G^0 is the

conductance under the carrier air flow. S was normalized taking into account the mass (m) of adsorbent, expressed in mg, (S/m) to enable a fair comparison of the preconcentration performance of each material. The testing parameters mentioned were optimized to detect all BTEX compounds simultaneously with the highest possible amplitude. The detection limit is defined as the minimum concentration at which BTEX can be reliably identified. In this study, we estimated the detection limit when the signal value is 3 times the noise ($S/N = 3$). As reference, the described detection method was also followed using a micro-preconcentrator without any deposited adsorbent.

3 Results and discussion

3.1 Understanding the pore structure of adsorbents

Figure 1 also displays transmission electronic microscopy (TEM) micrographs of both MMC adsorbents that confirm the ordered 2D hexagonal structure for OMC and the

disordered worm-like mesopore structure for DMC. On the other hand, Figure 2(a) shows the Ar adsorption–desorption isotherms on OMC and DMC materials. Concerning Ar adsorption, both MMCs exhibit a sharp Ar uptake at low relative pressures ($p/p_0 < 0.001$), confirming the existence of narrow micropores, and a “low-pressure hysteresis,” associated with an extremely tortuous micro-pore network [13]. Adsorption branches resulting from the combination of type Ia, typical of ultramicroporous materials, and type IVa, characteristic of mesoporous solids, were observed. The PSDs obtained from Ar and H_2 adsorption data are shown in Figure 2(b) and (c). Similar BET areas (A_{BET}) around $530 \text{ m}^2 \cdot \text{g}^{-1}$ and PSDs in the micropore range ($< 2 \text{ nm}$) were found due to the use of the same carbon precursor, tannin. Anticipated by the very different hysteresis cycles observed in Figure 2(a), the main PSD differences were observed in the mesopore range, see inset of Figure 2(b). OMC has a narrow peak centered at $\sim 5.5 \text{ nm}$, while DMC exhibits a broader peak centered at $\sim 5 \text{ nm}$ but extending from ca. 3 to 10 nm. Figure 2(c) shows the cumulated pore volume, in which mesopores represent 43 and 55% of the total pore volume for OMC and DMC, respectively.

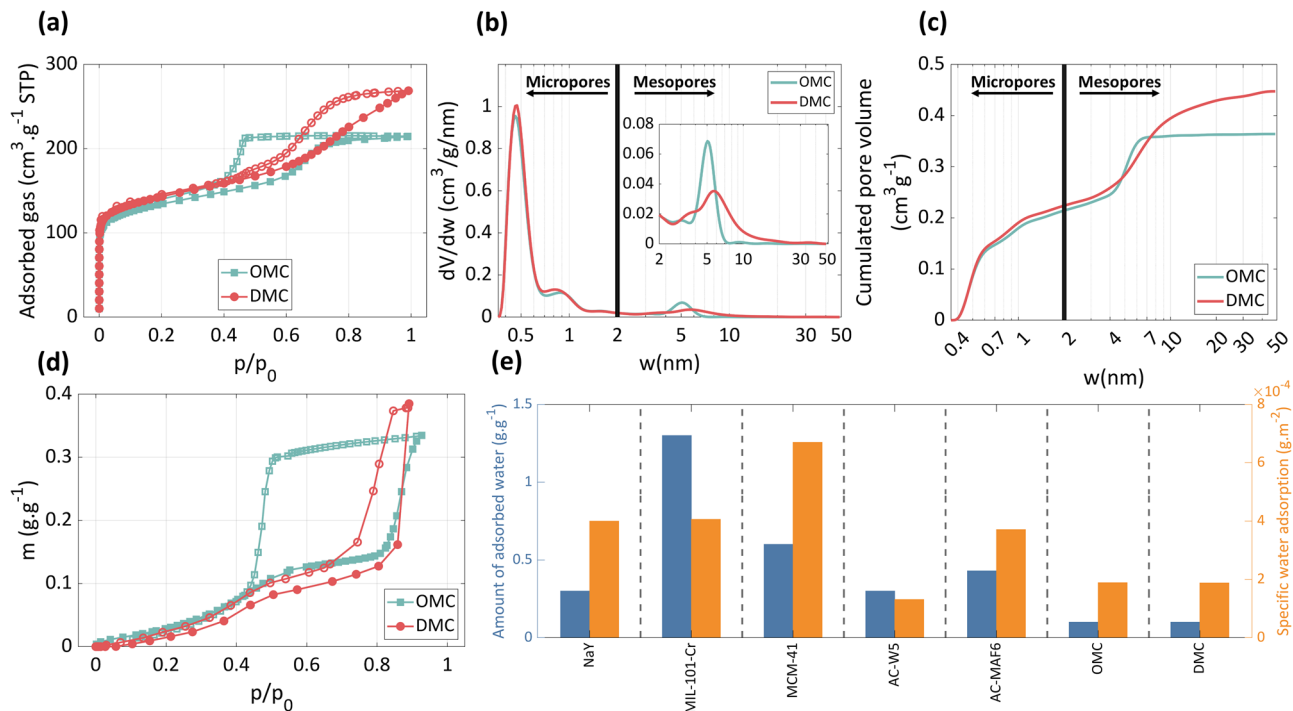


Figure 2: (a) Adsorption–desorption isotherms of Ar on OMC and DMC carbons at -186°C , full symbols: adsorption; empty symbols: desorption. (b) Differential and (c) cumulative PSDs obtained by applying the 2D NLDFT HS model to the Ar adsorption data. (d) Water adsorption–desorption isotherms on the MMCs materials at 25°C , full symbols: adsorption; empty symbols: desorption. (e) Amount of adsorbed water and specific water adsorption at $p/p_0 = 0.6$ for a series of porous materials (adapted from refs. [17,18]). p/p_0 : relative pressure, STP: Standard conditions for temperature and pressure, w : pore size.

3.2 Analyzing water adsorption at equilibrium

Since indoor air pollutants are always mixed with water vapor, we investigated the water adsorption isotherms at 25°C for each material (Figure 2(d)). Both MMCs adsorb a very low amount of water ($\sim 0.1 \text{ g}\cdot\text{g}^{-1}$) up to 60% RH ($p/p_0 \leq 0.6$ at 25°C), indicating that these materials are highly hydrophobic. For the sake of comparison, Figure 2(e) shows the specific ($\text{g}\cdot\text{g}^{-1}$) and surface ($\text{g}\cdot\text{m}^{-2}$) water adsorption capacities at $p/p_0 = 0.6$ for a range of porous materials, including a MOF (MIL-101-Cr), two zeolites (NaY and MCM41), and 2 ACs (AC-W5 and AC-MAF6), among them. Notably, Figure 2(e) clearly illustrates that our MMCs are among the most hydrophobic materials, making them ideal

candidates for the detection of VOCs at ppb concentration under real humidity conditions.

3.3 Evaluating preconcentration performance of adsorbents

We investigated the BTEX preconcentration performance of the MMCs using our μ -GC prototype. Figure 3(a) shows the normalized responses of the micro-system for the detection of 2.4 ± 0.1, 3.1 ± 0.1, 1.6 ± 0.1, 2.9 ± 0.1, and 2.5 ± 0.1 ppm of benzene, toluene, ethylbenzene, *p*-xylene, and *o*-xylene, respectively, in nearly dry air (2% RH at 25°C) and with a higher humidity condition of 60% RH at 25°C. As

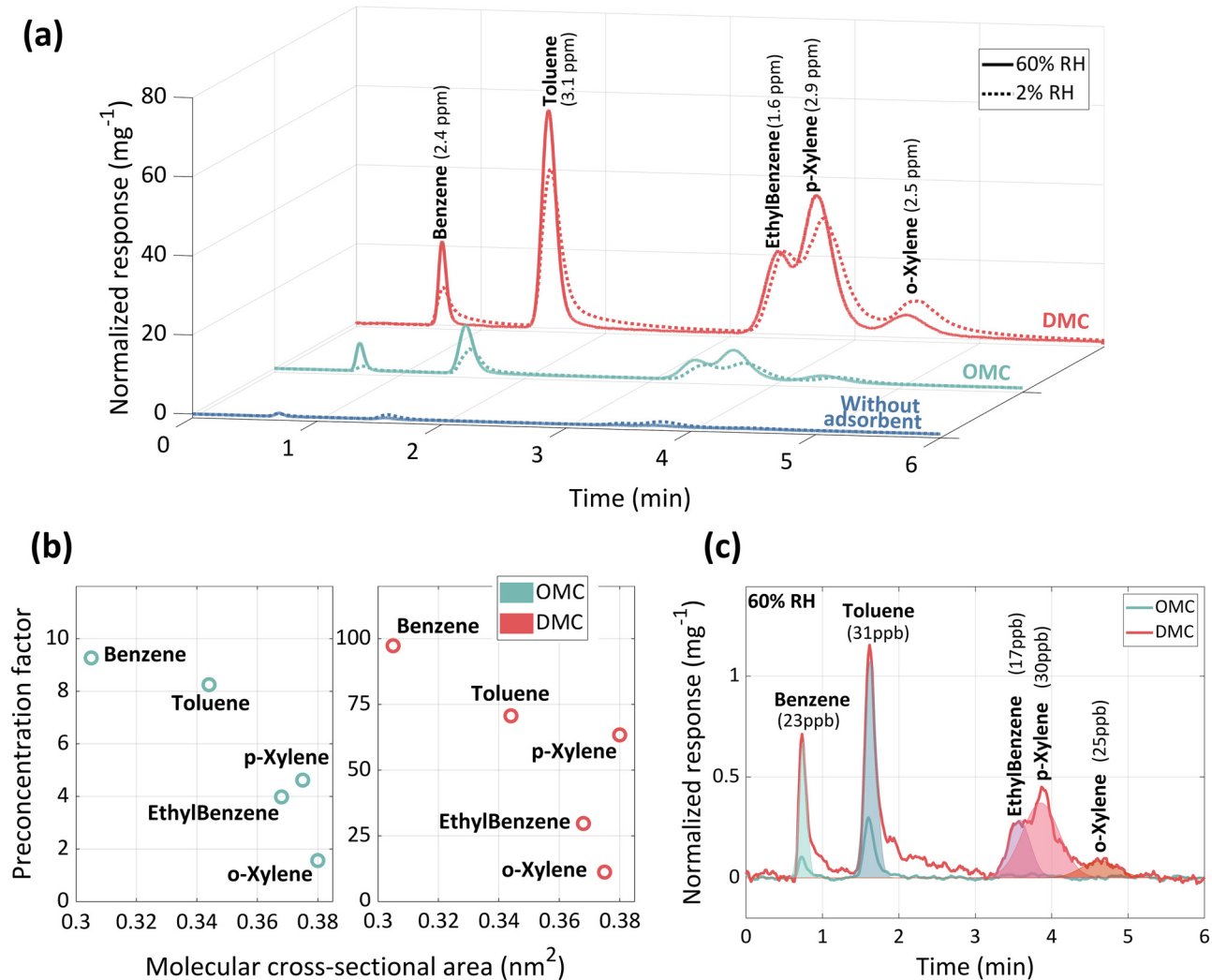


Figure 3: (a) Dynamic responses, normalized per milligram of adsorbent, of the micro-system for the detection of BTEX compounds in nearly dry air (2% RH at 25°C) and at 60% RH at 25°C; (b) PF of BTEX compounds for both adsorbents vs molecular cross-sectional area of species [20]; and (c) dynamic normalized responses for the detection of very low concentrations BTEX compounds under 60% RH at 25°C.

Table 1: Analytical figures of merit for BTEX detection using the DMC adsorbent under 60% RH at 25°C

Analytes	RT (s)	PF	Detection limit (ppb)	Linear regression	R ²	Linear range (ppb)	Repeatability (%)
Benzene	50 ± 5	96 ± 4	23 ± 5	$Y = 10.65X + 0.44$	0.999	(23–2,400)	4
Toluene	100 ± 5	68 ± 4	31 ± 5	$Y = 12.49X + 1.34$	0.998	(31–3,100)	4
Ethylbenzene	210 ± 5	29 ± 4	17 ± 5	$Y = 13.77X + 0.26$	0.999	(17–1,600)	5
p-Xylene	225 ± 5	62 ± 4	30 ± 5	$Y = 10.04X + 0.17$	0.999	(30–2,900)	5
o-Xylene	270 ± 5	13 ± 4	25 ± 5	$Y = 7.84X - 0.60$	0.995	(25–2,500)	5

RT: retention time; PF: preconcentration factor; R²: determination coefficient; Y and X correspond to the MOS gas sensor signal and the BTEX concentration, respectively; Repeatability was evaluated over 4 months with more than 300 tests involving the preconcentration and separation of BTEX.

expected, the μ-GC prototype was able to identify each BTEX compound, and its response was enhanced with the use of MMCs in the preconcentration unit.

The total analysis time, including the preconcentration sequence, was close to 10 min, which is a short time compared to conventional indoor air analysis techniques such as thermal desorption-GC/mass spectrometry where around 40 min is required for sampling and sorbent preconditioning, followed by an additional 40 min due to the use of longer GC columns that extend detection times of ~40 min [19]. The response of the micro-system was significantly enhanced when using DMC, surpassing the results obtained with OMC, indicating that DMC exhibits a superior preconcentration performance for BTEX.

The preconcentration factor (PF) is defined as the ratio of the height of a given peak when using an adsorbent and, in its absence, is also significantly greater for DMC compared to OMC (Figure 3(b)). It is noteworthy that the RH has little impact on the preconcentration performance since it is only slightly changed when increasing the RH from 2 to 60% at 25°C, confirming the hydrophobic nature of these MMCs and indicating that moisture does not significantly interfere with this specific application.

The normalized responses for several very low concentrations of mixed BTEX, under an adsorption time of 5 min at 60% RH at 25°C, are shown in Figure 3(c). DMC allowed the detection of each compound in the mixture at remarkably low concentrations, namely, 23 ± 5, 31 ± 5, 17 ± 5, 25 ± 5, and 30 ± 5 ppb of benzene, toluene, ethylbenzene, o-xylene, and p-xylene, respectively. It is worth noting that these concentrations are the lowest that our experimental

setup can generate. In contrast, OMC enabled benzene and toluene detection at concentrations of 23 ± 5 and 31 ± 5 ppb, respectively, but failed to detect ethylbenzene and xylene isomers at concentrations below 300 ppb. Hence, it can be observed that the detection limit is lower for DMC. More information on the analytical figures of merit is given in Table 1.

Considering the similarity in the surface chemical composition of the MMCs [14], their interactions with BTEX compounds should also be quite similar. Consequently, differences in detection can be ascribed to the size of the BTEX molecules, as shown in Table 2 [20].

Benzene, being the smallest molecule in the BTEX mixture with a cross-sectional area of 0.305 nm², diffuses more rapidly within the porous material and is, therefore, the molecule with the highest concentration factor. In contrast, xylene isomers, having a cross-sectional area between 0.375 nm² for o- and m-xylene and 0.380 nm² for p-xylene, diffuse less easily into the pores and are therefore less prone to be adsorbed than benzene, resulting in a smaller electrical signal from the gas sensor. Despite the higher kinetic diameter of p-xylene, the alignment of its two methyl groups and the benzene ring facilitates easier access of this compound to the pores of the adsorbent. This may also explain why the preconcentration capacities of p-xylene are significantly higher than those of o-xylene (Figure 3(b)).

In a previous study, immersion calorimetry experiments involving three C6 isomers, with kinetic diameters between 0.43 and 0.62 nm, were conducted on OMC and DMC, yielding significant insight into the pore network

Table 2: Cross-sectional area of BTEX molecules [20]

	VOCs				
	Benzene	Toluene	Ethylbenzene	o-Xylene	p-Xylene
Cross-sectional area (nm ²)	0.305	0.344	0.368	0.375	0.380

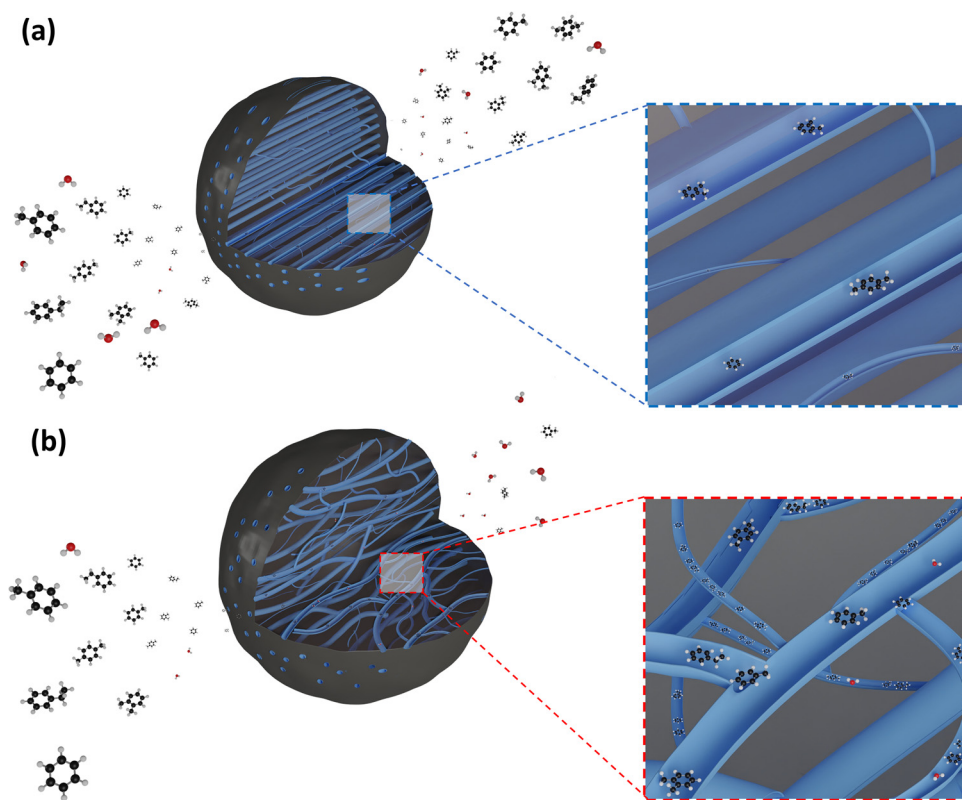


Figure 4: Illustration of the BTEX diffusion inside the micro-mesoporous network of (a) ordered and (b) disordered micro-mesoporous adsorbents.

connectivity of these MMCs [14]. They indicated that the constrictions connecting the mesoporous network of the OMC are slightly wider than 0.5 nm. Given the range of kinetic diameters exhibited by BTEX molecules, varying from 0.54 to 0.68 nm for benzene and *o*-xylene, respectively, BTEX adsorption on the OMC should be minimal, as confirmed by the low sensing responses of the microsystem. From these experimental results, a scheme of BTEX compound diffusion within a particle of OMC or DMC is illustrated in Figure 4. Within the well-ordered cylindrical mesoporous channels in OMC, access to the microporous surface is limited and few BTEX can be trapped inside, especially under dynamic conditions. On the contrary, BTEX compounds exhibit enhanced adsorption within the microporous structure of the DMC because diffusion is

facilitated by the well-connected pore network. This also explains why the PF is higher in DMC than in OMC, thus leading to very low LOD of each BTEX compound in DMC.

In addition, we conducted repeatability and stability tests, totaling over 300 tests involving thermal cycles. We observed a slight variation in the sensor signal (<5%), which we attribute to the expected drift of the commercial metal-oxide-based gas sensor. In the last decade, significant progress has been made in developing compact detection devices, yet there are limited reports in the literature on combining silicon-etched preconcentrators and GC micro-columns with metal oxide-based gas sensors for *in situ* detection of BTEX in humid air. Table 3 presents recent literature data on the sensing performances of various compact GC devices toward BTEX detection in air. It is

Table 3: Comparison with the literature

Detector*	Elution time of BTEX (min)	Concentration range of BTEX (ppb)	Humidity level
This work	MOS	~5	60% RH at 25°C
[21]	PID	12–20	30–50% at 25°C
[22]	Standard CMOS	~4 (benzene, toluene, <i>m</i> -xylene)	Dry air
[23]	PID	~20	Filtered air
[24]	PID	~16	Dry air

*MOS: metal oxide sensor; PID: photoionization detector; CMOS: complementary metal-oxide semiconductor.

important to note that most of the reported systems are not fully composed of silicon-integrated analytical units, unlike the prototype presented in this study. Table 3 shows that the sensing performance of our prototype is comparable to the best-performing systems reported in the literature.

4 Conclusion

In this study, we successfully synthesized tannin-derived MMCs and demonstrated their remarkable potential when integrated into a miniaturized preconcentration unit for the detection of VOCs in indoor air. Among the materials tested, the DMC exhibited exceptional performance, owing to its highly interconnected porous network. This unique structural connectivity significantly enhanced the accessibility of BTEX compounds (benzene, toluene, ethylbenzene, and xylene) to the micropores, resulting in unprecedented preconcentration efficiency, even under challenging real-world conditions.

DMC enabled the identification of 23 ± 5 , 31 ± 5 , 17 ± 5 , 25 ± 5 , and 30 ± 5 ppb of benzene, toluene, ethylbenzene, *o*-xylene, and *p*-xylene, respectively, within a short analysis time (~ 10 min), even in the presence of 60% RH at 25°C . Our findings highlight the transformative potential of DMC in environmental monitoring applications, particularly for indoor air quality assessment. The high pore connectivity within DMC enables it to function efficiently under conditions that typically challenge other adsorbent materials, making it a promising candidate for the development of advanced, sensitive detection systems. This work paves the way for future innovations in VOC detection technologies, where the design of adsorbent materials with optimized pore structures can lead to breakthroughs in environmental sensing and public health protection. Additional experiments involving a wider range of indoor air interferents are planned to better replicate real-world conditions.

Acknowledgments: This work was supported by the French RENATECH network and its FEMTO-ST technological facility. This work has been supported by the EIPHI Graduate School (contract ANR-17-EURE-0002) and the Region Bourgogne Franche-Comté. The authors acknowledge Blandine Guichardaz for her contribution to 3D carbon modeling.

Funding information: The UL authors gratefully acknowledge the support of the TALiSMAN [Grant Number 2019-000214] and TALiSMAN2 [Grant Number ERDF-LO0022687] projects, financed by the European Regional Development

Fund (ERDF), together with the UCGWATER+ project, financed by the Research Fund for Coal and Steel (RFCS) [Grant Agreement No 101033964].

Author contributions: All authors have accepted responsibility for the entire content of this manuscript and approved its submission.

Conflict of interest: Vanessa Fierro, who is the co-author of this article, is a current Editorial Board member of *Reviews on Advanced Materials Science*. This fact did not affect the peer-review process. The authors state no other conflict of interest.

Data availability statement: All data generated or analyzed during this study are included in this published article.

References

- [1] Loomis, D., K. Z. Guyton, Y. Grosse, F. El Ghissassi, V. Bouvard, L. Benbrahim-Tallaa, et al. Carcinogenicity of benzene. *The Lancet Oncology(London)*, Vol. 18, 2017, pp. 1574–1575.
- [2] Raysoni, A. U., T. H. Stock, J. A. Sarnat, M. C. Chavez, S. E. Sarnat, T. Montoya, et al. Evaluation of VOC concentrations in indoor and outdoor microenvironments at near-road schools. *Environmental Pollution*, Vol. 231, 2017, pp. 681–693.
- [3] Parra, M. A., D. Elustondo, R. Bermejo, and J. M. Santamaría. Quantification of indoor and outdoor volatile organic compounds (VOCs) in pubs and cafés in Pamplona, Spain. *Atmospheric Environment*, Vol. 42, 2008, pp. 6647–6654.
- [4] Zhong, L., F. C. Su, and S. Batterman. Volatile organic compounds (VOCs) in conventional and high performance school buildings in the U.S. *International Journal of Environmental Research and Public Health*, Vol. 14, No. 1, 2017, id. 100.
- [5] Lara-Ibeas, I., A. Rodríguez-Cuevas, C. Andrikopoulou, V. Person, L. Baldas, S. Colin, et al. Sub-ppb level detection of BTEX gaseous mixtures with a compact prototype GC equipped with a preconcentration unit. *Micromachines*, Vol. 10, 2019, id. 187.
- [6] Sun, J., N. Xue, W. Wang, H. Wang, C. Liu, T. Ma, et al. Compact prototype GC-PID system integrated with micro PC and micro GC column. *Journal of Micromechanics and Microengineering*, Vol. 29, 2019, id. 035008.
- [7] Chappuis, T. H., B. A. P. Ho, M. Ceillier, F. Ricoul, M. Alessio, J. F. Beche, et al. Miniaturization of breath sampling with silicon chip: application to volatile tobacco markers tracking. *Journal of Breath Research*, Vol. 12, 2018, id. 046011.
- [8] You, D. W., Y. S. Seon, Y. Jang, J. Bang, J. S. Oh, and K. W. Jung. A portable gas chromatograph for real-time monitoring of aromatic volatile organic compounds in air samples. *Journal of Chromatography A*, Vol. 1625, 2020, id. 461267.
- [9] Megías-Sayago, C., I. Lara-Ibeas, Q. Wang, S. Le Calvé, and B. Louis. Volatile organic compounds (VOCs) removal capacity of ZSM-5 zeolite adsorbents for near real-time BTEX detection. *Journal of Environmental Chemical Engineering*, Vol. 8, 2020, id. 103724.

[10] Dizbay-Onat, M., E. Floyd, U. K. Vaidya, and C. T. Lungu. Applicability of industrial sisal fiber waste derived activated carbon for the adsorption of volatile organic compounds (VOCs). *Fibers and Polymers*, Vol. 19, 2018, pp. 805–811.

[11] Isinkaralar, K., G. Gullu, and A. Turkyilmaz. Optimal preparation of low-cost activated carbon: the enhanced mechanism of interaction and performance studies for volatile organic compounds (VOCs) capture. *Biomass Conversion and Biorefinery*, Vol. 13, 2023, pp. 4279–4289.

[12] El Mohajir, A., J. Castro-Gutiérrez, R. Luan Sehn Canevesi, I. Bezverkhyy, G. Weber, J. P. Bellat, et al. Novel porous carbon material for the detection of traces of volatile organic compounds in indoor air. *ACS Applied Materials & Interfaces*, Vol. 13, No. 33, 2021, pp. 40088–40097.

[13] Castro-Gutiérrez, J., A. Sanchez-Sánchez, J. Ghanbaja, N. Díez, M. Sevilla, A. Celzard, et al. Synthesis of perfectly ordered mesoporous carbons by water-assisted mechanochemical self-assembly of tannin. *Green Chemistry*, Vol. 20, 2018, pp. 5123–5132.

[14] Castro-Gutiérrez, J., E. De Oliveira Jardim, R. L. S. Canevesi, J. Silvestre-Albero, M. Kriesten, M. Thommes, et al. Molecular sieving of linear and branched C6 alkanes by tannin-derived carbons. *Carbon*, Vol. 174, 2021, pp. 413–422.

[15] Thommes, M., K. Kaneko, A. V. Neimark, J. P. Olivier, F. Rodriguez-Reinoso, J. Rouquerol, et al. Physisorption of gases, with special reference to the evaluation of surface area and pore size distribution (IUPAC Technical Report). *Pure and Applied Chemistry. Chimie pure et appliquée*, Vol. 87, 2015, pp. 1051–1069.

[16] Gregis, G., J. B. Sanchez, I. Bezverkhyy, G. Weber, F. Berger, V. Fierro, et al. Detection and quantification of lung cancer biomarkers by a micro-analytical device using a single metal oxide-based gas sensor. *Sensors and Actuators B, Chemical*, Vol. 255, 2018, pp. 391–400.

[17] Pujol, Q., G. Weber, J. P. Bellat, S. Gratz, A. Krusenbaum, L. Borchardt, et al. Potential of novel porous materials for capture of toluene traces in air under humid conditions. *Microporous and Mesoporous Materials*, Vol. 344, 2022, id. 112204.

[18] Zhao, W., V. Fierro, N. Fernandez-Huerta, M. T. Izquierdo, and A. Celzard. Impact of synthesis conditions of KOH activated carbons on their hydrogen storage capacities. *International Journal of Hydrogen Energy*, Vol. 37, 2012, pp. 14278–14284.

[19] Kaikiti, C., M. Stylianou, and A. Agapiou. TD-GC/MS analysis of indoor air pollutants (VOCs, PM) in hair salons. *Chemosphere*, Vol. 294, 2022, id. 133691.

[20] Yang, K., Q. Sun, F. Xue, and D. Lin. Adsorption of volatile organic compounds by metal–organic frameworks MIL-101: Influence of molecular size and shape. *Journal of Hazardous Materials*, Vol. 195, 2011, pp. 124–131.

[21] Frausto-Vicencio, I., A. Moreno, H. Goldsmith, Y. K. Hsu, and F. M. Hopkins. Characterizing the performance of a compact BTEX GC-PID for near-real time analysis and field deployment. *Sensors*, Vol. 21, 2021, id. 2095.

[22] Tzeng, T. H., C. Y. Kuo, S. Y. Wang, P. K. Huang, Y. M. Huang, and W. C. Hsieh. A portable micro gas chromatography system for lung cancer associated volatile organic compound detection. *IEEE Journal of Solid-State Circuits*, Vol. 51, 2016, pp. 259–272.

[23] Skog, K. M., F. Xiong, H. Kawashima, E. Doyle, R. Soto, and D. R. Gentner. Compact, automated, inexpensive, and field-deployable vacuum-outlet gas chromatograph for trace-concentration gas-phase organic compounds. *Analytical Chemistry*, Vol. 91, No. 2, 2019, pp. 1318–1327.

[24] Rodríguez-Cuevas, A., I. Lara-Ibeas, A. Leprince, M. Wolf, and S. Le Calvé. Easy-to-manufacture micro gas preconcentrator integrated in a portable GC for enhanced trace detection of BTEX. *Sensors and Actuators B, Chemical*, Vol. 324, 2020, id. 128690.